THE ARCHIVES OF TRANSPORT

VOL. XXIII NO 1 2011

10.2478/v10174-011-0006-9

State – Space Control of the Drive with PMSM and Flexible Coupling

Ján Vittek*
Pavol Makyš*
Milan Pospíšil*
Elżbieta Szychta**
Mirosław Luft**

Received January 2011

Abstract

A control system, which achieves prescribed speed and position responses, for electric drives with a significant torsion vibration mode is presented. Control system design exploits state-space control and forced dynamics control principles. Derived control algorithm respects the vector control condition by keeping the direct axis current component approximately zero as well as controlling the load position with prescribed closed loop dynamics. Set of two observers, one on load side and the second one on motor side, generate all state variables necessary for control algorithm design including torques acting on the motor and load side to satisfy all conditions for achieving prescribed dynamics. This approach eliminates the position sensor on motor side. The simulations confirm that proposed model based position control system can operate with moderate accuracy.

Keywords: control systems, control vector algorithm, state-space control

1. Introduction

To reduce number of sensors for position control of the drive with flexible coupling a control system based on state-space control and forced dynamics con-

* University of Zilina, Faculty of Electrical Engineering, SLOVAKIA; 010 26 Zilina; Univerzitna 1, 29, e-mail: jan.vittek@fel.uniza.sk

** Technical University of Radom, Faculty of Transport and Electrical Engineering, POLAND; Radom 26-600; Malczewskiego 29, e-mail: e.szychta@pr.radom.pl

trol completed with observation of state variables is developed. Main goal here is to verify overall position control algorithm together with correct function of two observers mutually interacted providing estimates of all the necessary state-space variables for control including of load torques on both sides of flexible coupling.

Control algorithm for state-space control of load position, θ_L of the drive with permanent magnet synchronous motor (PMSM) and flexible coupling is developed in two consequent steps.

First an inner motor speed control loop is formed using feedback linearisation principles, [1]. This control algorithm is formulated in the rotor flux fixed d_q frame respecting mutual orthogonality of the stator current vector and rotor magnetic flux vector to achieve maximum torque of the machine, [2, 3]. Applying 'Forced Dynamics Control,' (FDC) principles, [4] speed control system responses with prescribed linear first order dynamic with specified time constant, T. Speed control system also automatically counteracts motor load torque by producing a nearly equal and opposite control torque component, provided by motor torque observer.

State-space position control system including state-feedback completed with integral controller is developed as second step. Replacement of the whole speed control loop with the first order delay not only linearises this loop but also substantially simplifies design of the overall position control system. Design of position control algorithm exploits FDC principles and therefore complies also with prescribed closed-loop dynamics for load angle control in spite of the external load torque and the vibration mode presence. This approach achieves non-oscillatory position control with a specified settling time, T_{ss}.

Even if state-space control principles are exploited the calculation of state feedbacks coefficients and integral controller constant is done by pole-placement method. Possibility to exploit FDC for control of the drive with flexible coupling was already verified in [5]. Designed control system there requires two position sensors. One sensor is used to measure rotor position and the second one measures load position. Preliminary experiments with this control structure confirm possibility to control load angle with prescribed dynamics. Conventional approach to control of the drive with flexible coupling with PI and PID regulators designed by pole-placement method for speed control of two inertia system was described in [6].

Linearisation of the speed control algorithm and the design state-space based position control algorithm operating with one position sensor only require estimation of state variables including load torques. To complete this task two observers were designed. Due to state dependence of flexible load the observer on load side is designed as state observer. Second observer on motor side is Luenberger type and its main purpose is to estimate for FDC torque acting on the shaft of motor.

The original contribution of this paper is a preliminary verification by simulation of proper function of the overall control system including two observers. Simulation results presented further confirm that control system and observers operates in agreement with theoretical assumptions made under their development and design

control system is capable to eliminate the torsion oscillations while controlling the load position with moderate precision.

2. Position Control System Development

Basic idea of the position control system development is at first to linearised control system for speed control of the PMSM and secondly to design state-space position control system, which obtains all the state variables from state-space observer based on the load model.

Overall position control system block diagram is shown in Fig. 1. If compared with [5], designed control system needs the measurement of load position only. This way elimination of position sensor on the side of PMSM is achieved.

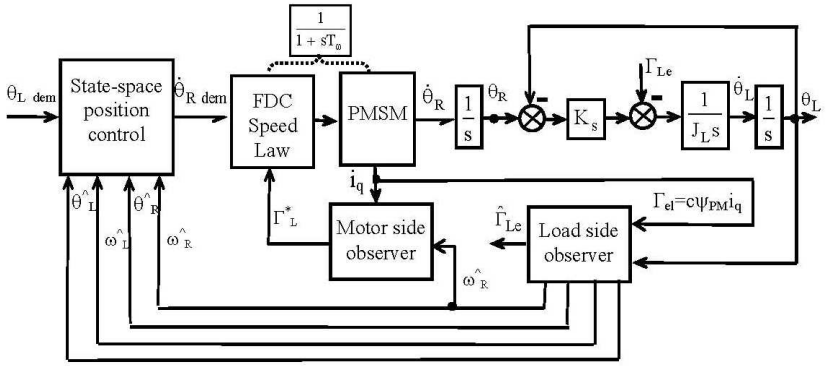

Fig. 1. Block diagram for position control system design

2.1. Description of PMSM and Load

The PMSM is described in the synchronously rotating d_q co-ordinate system fixed to the rotor of PMSM:

$$\frac{d\theta_R}{dt} = \omega_R, \tag{1}$$

$$\frac{d\omega_R}{dt} = \frac{1}{J}\left\{c\left[\Psi_{PM}i_q + \left(L_d - L_q\right)i_d\, i_q\right] - \Gamma_L\right\}, \tag{2}$$

$$\frac{di_d}{dt} = \frac{-R_s}{L_d}i_d + p\omega_R\frac{L_q}{L_d}i_q + \frac{1}{L_d}u_d, \tag{3}$$

$$\frac{di_q}{dt} = \frac{-R_s}{L_q}i_q - p\omega_R\frac{L_d}{L_q}i_d - \frac{p\omega_R}{L_q}\Psi_{PM} + \frac{1}{L_q}u_q, \tag{4}$$

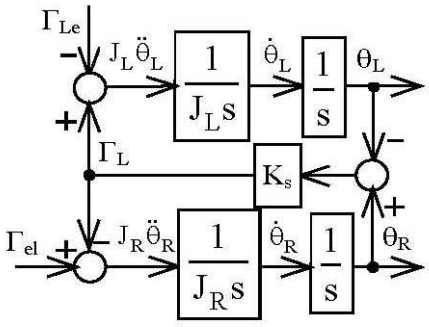

Fig. 2. Representation of the flexible coupling

where i_d, i_q and u_d, u_q are, respectively, the stator current and voltage components, θ_R and ω_R are the rotor position and angular velocity respectively and Γ_L is the external motor torque, p is the number of pole pairs and c=3p/2.

Fig. 2 shows flexible coupling representation and the differential equations, where K_s is spring constant, are as follow:

$$\dot{\theta}_L = \omega_L, \tag{5}$$

$$\ddot{\theta}_R = \frac{1}{J_R}\left[\Gamma_{el} - \Gamma_L\right], \quad \text{where} \quad \Gamma_L = K_s\left(\theta_R - \theta_L\right), \tag{6}$$

$$\ddot{\theta}_L = \frac{1}{J_L}\left[\Gamma_L - \Gamma_{Le}\right]. \tag{7}$$

2.2. FDC of Motor Speed

The rotor speed is modeled by (2), where J_R is the rotor moment of inertia. The FDC speed law for rotor is based on the feedback linearisation that yields the first order linear dynamics, where T_ω is the prescribed time constant and ω_{Rdem} is the demanded rotor speed.

$$\frac{d\omega_R}{dt} = \frac{1}{T_\omega}\left(\omega_{R\,dem} - \omega_R\right) \quad \text{or} \quad \ddot{\theta}_R = \frac{1}{T_\omega}\left(\dot{\theta}_{R\,dem} - \dot{\theta}_R\right). \tag{8a,b}$$

Setting i_d=0 up to nominal speed for vector control of the PMSM, [3] and equating the RHS of (2) and (8b) yields the following FDC law for PMSM inner speed control loop:

$$i_{d\,dem} = 0 \tag{9}$$

$$i_{q\,dem} = \frac{1}{c\Psi_{PM}}\left[\frac{J_r}{T_\omega}\left(\dot{\theta}_{R\,dem} - \dot{\theta}_R\right) + \Gamma_L\right], \tag{10}$$

hence $i_d=i_{d\,dem}$ and $i_q=i_{q\,dem}$ are regarded as the control variables. Current controlled inverter is used to vary the stator voltage components, u_d and u_q, such a way that stator components i_d and i_q follow their respective demands, $i_{d\,dem}$ and $i_{q\,dem}$, with zero dynamic lag.

Since the load torque appears on the right hand side of the demanded current, $i_{q\,dem}$, (8) it is necessary to design an observer for estimation of the net load torque acting on the shaft of the motor (*see corresponding section 3.2*). Derived equations (9) and (10) are used for FDC of PMSM rotor speed with the first order dynamics and prescribed settling time, T_ω This way speed controlled PMSM was linearised and for the design of position control loop will be replaced with simple first order delay.

2.3. Design of State-space Load Position Control

Plant for position control is formed by first replacing the FDC speed control loop of PMSM by its ideal first order transfer function block and then integrating this block with the model of load. The resulting plant for position control loop of load angle is shown in Fig. 4.

Coefficients for state feedback and integral controller constant for position control system shown as Fig. 3, are designed using pole placement method.

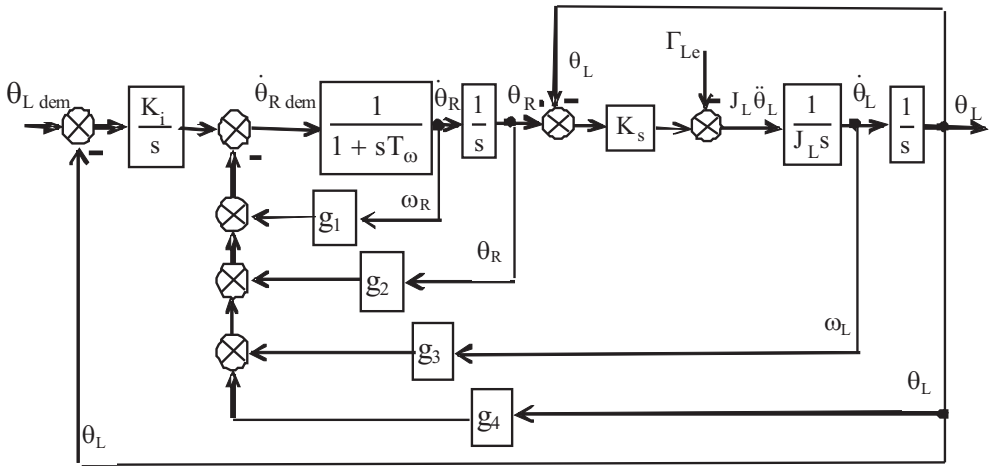

Fig. 3. Block diagram for position control system design

First the transfer function of position control system was expressed as:

$$F(s)=\frac{\theta_L(s)}{\theta_{L\,dem}(s)}=\frac{\dfrac{K_iK_s}{J_LT_\omega}}{s^5+s^4\dfrac{1+g_1}{T_\omega}+s^3\dfrac{g_2J_L+K_sT_\omega}{J_LT_\omega}+s^2\dfrac{K_s}{J_LT_\omega}(1+g_3)+s\dfrac{K_sg_4}{J_LT_\omega}+\dfrac{K_iK_s}{J_LT_\omega}} \tag{11}$$

Transfer function was compared with desired polynomial with multiple poles respecting Dodds settling time formula, [7] (*time to achieve 95% of demanded steady-state value*):

$$T_{ss} = 1,5\,(1+n)\frac{1}{\omega_n} \quad \text{or} \quad \omega_n = 1,5\,(1+n)\,\frac{1}{T_{ss}} \tag{12ab}$$

where ω_n is natural frequency of the system and n is order of the system. Desired polynomial then has form:

$$(s+\omega_n)^5 = s^5 + 5\omega_n s^4 + 10\omega_n^2 s^3 + 10\omega_n^3 s^2 + 5\omega_n^4 s + \omega_n^5 \tag{13}$$

Comparing the coefficients of the same degree in (11) and (13) yields the required values of integration constant, K_i and state-feedback gains, g_i i=1,2,3,4 as:

$$\begin{aligned} &K_i = \omega_n^5 \frac{J_L T_\omega}{K_s}, \quad g_4 = 5\omega_n^4 \frac{J_L T_\omega}{K_s}, \quad g_3 = 10\omega_n^{34} \frac{J_L T_\omega}{K_s} - 1, \\ &g_2 = T_\omega \left(10\omega_n^2 - \frac{K_s}{J_L}\right), \quad g_1 = 5\omega_n T_\omega - 1 \end{aligned} \tag{14}$$

3. Design of Observers

3.1. Load-side Observer

Due to state dependence of the shaft deflection torque, Γ_L the '*load side observer*' is based on a real time model of the two-mass system, where Γ_{Le} is an external load torque. In this case the external torque is treated as if it is constant provided that its change over a period equal to the observer correction loop settling time, T_{sO}, is negligible. The observer correction loops are actuated by the error, $e_\theta = \theta_L - \theta_L^\wedge$, between the measured load position and its estimate from the observer.

The observer state equations are therefore as follows:

$$sp_L = \omega_L, \tag{15}$$

$$sp_R = \omega_R, \tag{16}$$

$$s\omega_L = -\frac{K_s}{J_L} p_L + \frac{K_s}{J_L} p_R - \frac{1}{J_L}\Gamma_{Le}, \tag{17}$$

$$s\omega_R = \frac{K_s}{J_R} p_L - \frac{K_s}{J_R} p_R + \frac{1}{J_R}\Gamma_{el} \tag{18}$$

$$s\Gamma_{Le} = 0. \tag{19}$$

Following constants are defined, $a_1=K_s/J_L$, $a_2=1/J_L$, $a_3=K_s/J_R$ and $a_4=1/J_R$ for real time system matrix form description:

$$\begin{bmatrix} \dot{p}_L \\ \dot{p}_R \\ \dot{\omega}_L \\ \dot{\omega}_R \\ \dot{\Gamma}_{Le} \end{bmatrix} = \begin{bmatrix} 0 & 0 & 1 & 0 & 0 \\ 0 & 0 & 0 & 1 & 0 \\ -a_1 & a_1 & 0 & 0 & -a_2 \\ a_3 & -a_3 & 0 & 0 & 0 \\ 0 & 0 & 0 & 0 & 0 \end{bmatrix} \begin{bmatrix} p_L \\ p_R \\ \omega_L \\ \omega_R \\ \Gamma_{Le} \end{bmatrix} + \begin{bmatrix} 0 \\ 0 \\ 0 \\ a_4 \\ 0 \end{bmatrix} \Gamma_{el}. \tag{20}$$

If the error, $e_0=p_L - p_L^{\wedge}$ between the measured load position and its estimate multiplied with proper gain is added into each equation then observer equations written in matrix form are:

$$\begin{bmatrix} \hat{\dot{p}}_L \\ \hat{\dot{p}}_R \\ \hat{\dot{\omega}}_L \\ \hat{\dot{\omega}}_R \\ \hat{\dot{\Gamma}}_{Le} \end{bmatrix} = \begin{bmatrix} 0 & 0 & 1 & 0 & 0 \\ 0 & 0 & 0 & 1 & 0 \\ -a_1 & a_1 & 0 & 0 & -a_2 \\ a_3 & -a_3 & 0 & 0 & 0 \\ 0 & 0 & 0 & 0 & 0 \end{bmatrix} \begin{bmatrix} \hat{p}_L \\ \hat{p}_R \\ \hat{\omega}_L \\ \hat{\omega}_R \\ \hat{\Gamma}_{Le} \end{bmatrix} + \begin{bmatrix} 0 \\ 0 \\ 0 \\ a_4 \\ 0 \end{bmatrix} \Gamma_{el} + \begin{bmatrix} k_{p1} \\ k_{p2} \\ k_{\omega 1} \\ k_{\omega 2} \\ k_{\Gamma 1} \end{bmatrix} (p_L - \hat{p}_L) \tag{21}$$

By subtracting of observer equations from its real time model equation the dynamical error system has form:

$$\begin{bmatrix} \dot{\varepsilon}_{pL} \\ \dot{\varepsilon}_{pR} \\ \dot{\varepsilon}_{\omega L} \\ \dot{\varepsilon}_{\omega R} \\ \dot{\varepsilon}_{\Gamma_{Le}} \end{bmatrix} = \begin{bmatrix} -k_{p1} & 0 & 1 & 0 & 0 \\ -k_{p2} & 0 & 0 & 1 & 0 \\ -a_1 - k_{\omega 1} & a_1 & 0 & 0 & -a_2 \\ a_3 - k_{\omega 2} & -a_3 & 0 & 0 & 0 \\ k_{\Gamma 1} & 0 & 0 & 0 & 0 \end{bmatrix} \begin{bmatrix} \varepsilon_{pL} \\ \varepsilon_{pR} \\ \varepsilon_{\omega L} \\ \varepsilon_{\omega R} \\ \varepsilon_{\Gamma_{Le}} \end{bmatrix} \tag{22}$$

To ensure convergence of the state estimates toward the real states the gains of observer, k_{p1}, k_{p2}, $k_{\omega 1}$, $k_{\omega 2}$ and $k_{\Gamma 1}$ must be chosen such way that dynamical error system satisfies condition for $t\rightarrow \infty$ $\varepsilon_i(t)\rightarrow 0$. Such convergence is guaranteed if the eigenvalues of the system matrix have negative real parts.

$$\det \begin{bmatrix} k_{p1} + \lambda & 0 & -1 & 0 & 0 \\ k_{p2} & \lambda & 0 & -1 & 0 \\ a_1 + k_{\omega 1} & -a_1 & \lambda & 0 & a_2 \\ a_3 - k_{\omega 2} & a_3 & 0 & \lambda & 0 \\ -k_{\Gamma 1} & 0 & 0 & 0 & \lambda \end{bmatrix} = \begin{array}{c} \lambda^5 + \lambda^4 k_{p1} + \lambda^3 (1 + a_1 + k_{\omega 1}) + \\ + \lambda^2 \left(k_{p1} + a_1 k_{p2} + k_{\Gamma 1} a_2\right) + \\ + \lambda \left[a_3 (a_1 + k_{\omega 1}) + a_1 (k_{\omega 2} - a_3)\right] + \\ + a_2 a_3 k_{\Gamma 1} \end{array} \tag{23}$$

Under assumption of collocations of all five dynamical error system eigenvalues at λ=-ω_0 (*the observers settling time can be determined by Dodds formula, (12a), which for n=5 results in* $T_{sO} = 9/\omega_0$). The desired characteristic equation has form:

$$(s + \omega_0)^5 = s^5 + 5\omega_0 s^4 + 10\omega_0^2 s^3 + 10\omega_0^3 s^2 + 5\omega_0^4 s + \omega_0^5 \tag{24}$$

Comparing the coefficients of the same degree in (23) and (24) yields the required values of observer gains:

$$\begin{aligned} &k_{\Gamma 1} = \frac{\omega_0^5}{a_2 a_3}, \quad k_{p1} = 5\omega_0, \quad k_{\omega 1} = 10\omega_0^2 - a_1 - 1, \\ &k_{p2} = \left(10\omega_0^3 - k_{p1} - k_{\Gamma 1} a_2\right)/a_1, \quad k_{\omega 2} = \left(5\omega_0^4 - a_3 k_{\omega 1}\right)/a_1. \end{aligned} \tag{25}$$

Although the load torque is assumed constant in the formulation of observer real time model, the estimate of this torque, $\Gamma_{Le}^{\wedge}$, will follow a time varying load torque and will do so more faithfully as ω_0 is enlarged with respect of computational step. Block diagram of motor side observer is shown in Fig. 4.

3.2. Motor-side Observer

Load torque on the motor shaft needs to be estimated in '*motor side observer*'. Due to fact that the form of $\Gamma_L(t)$ is unknown, its differential equations cannot be formed. Motor load torque, Γ_L is therefore treated as state variable, which is constant provided that its change over a period equal to the observer correction loop settling time, T_{so}, is negligible. So with sufficiently small settling time of observer, T_{so}, the observer produces a net load torque estimate, $\Gamma_L^*(t)$ able to track real load torque, $\Gamma_L(t)$, with very small and defined dynamic lag. Thus, the observer real time model is based on (1) and (2) augmented by a new state equation, $-d\Gamma_L/dt = 0$. The observer correction loops are actuated by the error, $e_\theta^* = \theta_r^{\wedge} - \theta_r^*$, between the estimated position from load side observer and its new estimate from the motor side observer. Block diagram of motor side observer is shown in Fig. 5.

The observer state equations are therefore as follows:

$$\frac{d\theta_R^*}{dt} = \omega_R^* + k_\theta e_\theta^*, \tag{26}$$

$$\frac{d\omega_R^*}{dt} = \frac{1}{J_R}\left(c\Psi_{PM} i_q - \hat{\Gamma}_L\right) + k_\omega e_\theta^*, \tag{27}$$

$$\frac{-d\Gamma_L^*}{dt} = 0 + k_\Gamma e_\theta^*. \tag{28}$$

Here, k_θ, k_ω nd k_Γ are the observer's correction loop gains, which can be designed by pole placement method. Characteristic polynomial of the observer's transfer function has form:

$$s^3 + k_\theta s^2 + k_\omega s + \frac{k_\Gamma}{J_R} \tag{29}$$

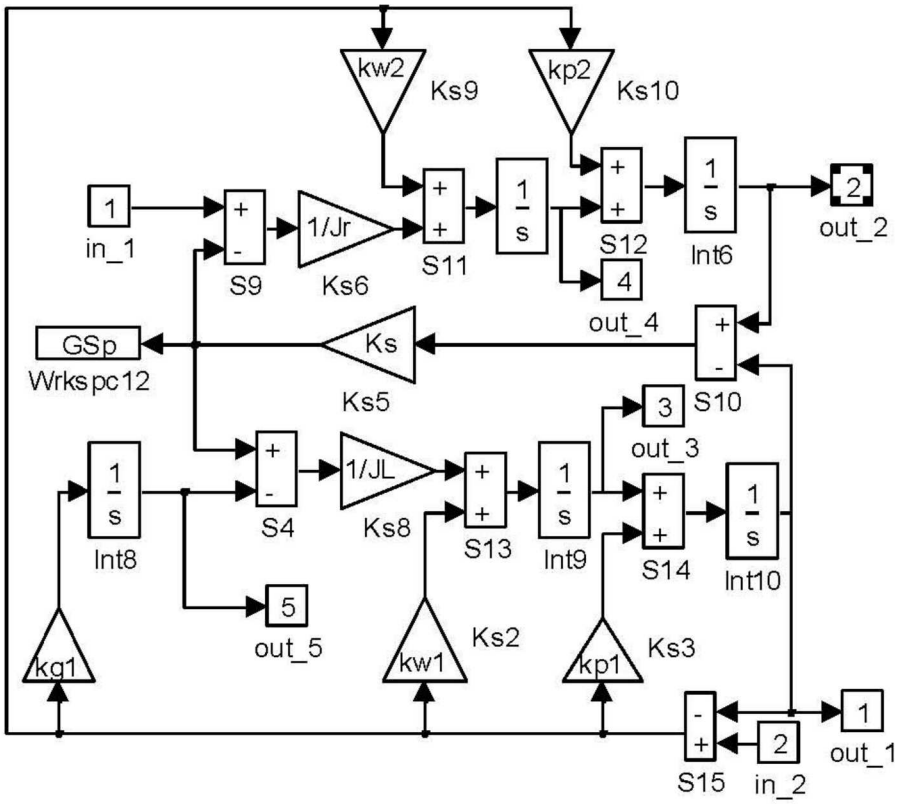

Fig. 4. Block diagram of load side observer in Simulink

Under assumption of collocations of all three observers poles at $\lambda=-\omega_0$ the settling time formula (12) can be used to determine natural frequency of observer, ω_0, which for n=3 results in $\omega_0 = 6/T_{so}$. The desired characteristic equation has form:

$$\left(s + \frac{6}{T_{so}}\right)^3 = s^3 + s^2\frac{18}{T_{so}} + s\frac{108}{T_{so}^2} + \frac{216}{T_{so}^3} \tag{30}$$

and yields a correction loop settling time, T_{so} (*defined as the time taken for* $|e_\theta(t)|$ *to fall to and stay below 5% of its peak value following a disturbance*). Comparing the coefficients of the same degree in (29) and (30) then yields the required values of observer gains for the chosen settling time, T_{so}.

$$k_\theta = \frac{18}{T_{so}}, \quad k_\omega = \frac{108}{T_{so}^2}, \quad k_\Gamma = \frac{216J_r}{T_{so}^3}. \tag{31}$$

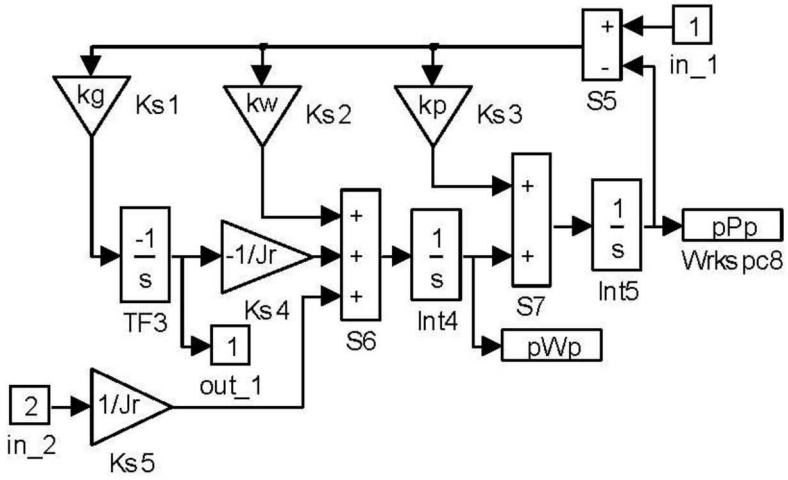

Fig. 5. Block diagram of motor side observer in Simulink

In spite of constant motor load torque assumed during observer real time model formulation its estimate, Γ_L, will follow a time varying motor load torque as faithfully as observer settling time, T_{so} is reduced.

4. Verification by Simulation

Block diagram of overall control system for position control of the drive with flexible coupling in Matlab-Simulink is shown in Fig. 6.

The simulation results for position control of the drive with flexible coupling are presented in Fig. 7. Computational step is h=1e-4 s, which corresponds to the sampling frequency achieved during a previous implementation of the FDC algorithm for position control. All the simulations are carried out with zero initial state variables and a step load position demand, $\theta_{L\ dem}$ =6,28 radians and a prescribed settling time of T_{ss}=0,1 s.

An external load torque was simulated as a sinus function, $\Gamma_{Le} = \Gamma_{max} \sin \omega_L t$, where Γ_{max}=1 Nm, ω_L=20 s^{-1}. This torque was applied at t=0,6 s, being zero for the time interval t<0,6 s. The settling time of the speed control loop, T_ω was prescribed as $T_\omega = T_{ss}/2$, while settling time of both observers was equal and set as $T_{so}=T_{sO}=0{,}1T_{ss}$. Moments of inertia of motor and load were equal, $J_L=J_R=0{,}0015$ kgm^2, while spring constant K_s=24 Nm/rad.

Subplot (a) shows the ideal position response computed from prescribed transfer function (11) together with a real response of the control system to the step position demand, θ_{dem}=6,28 rad, including error between them magnified 2 times. As can be seen observed and real position response show significant, though not very large, departure from the ideal performance, which is due to mainly non-zero iteration

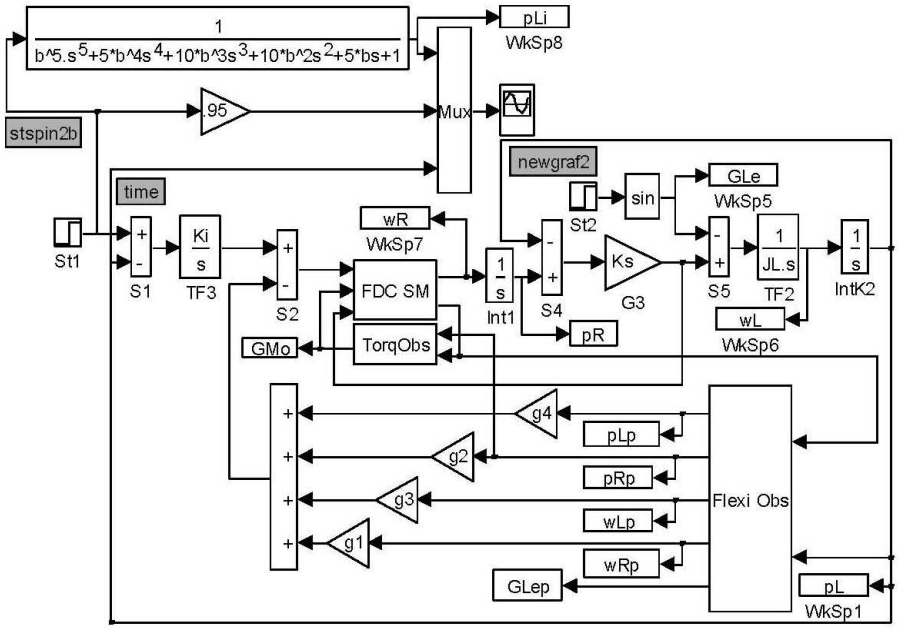

Fig. 6. Overall position control system block diagram in Simulink

interval as well as time delays in motor torque estimation. A torsion deflection of the spring is evident from time function of rotor angle, θ_R in subplot (b), where the oscillations with occur immediately after start-up of the drive and also for t>0,6 s when sinusoidal oscillations with ω_L=20 s^{-1} due to applied load torque are visible. Subplot (b) also shows an estimated rotor speed, $\theta_R^{\wedge}$ from load side observer including error between them magnified 10 times.

Subplot (c) shows the angular velocity of the load, ω_L together with its estimate, $\omega_L^{\wedge}$ and error between them magnified 10 times. Both functions are indicating that the acceleration period is followed by the deceleration period, as expected. Oscillations due to compensation of spring deflection during transients together with oscillations in steady state compensating applied load torque are clearly seen from function of rotor speed, ω_R in subplot (d). This subplot also contains the estimate of rotor speed, $\omega_R^{\wedge}$ together with their error magnified 10 times confirming correct function of load side observer. Electrical torque, Γ_{el} together with its estimate, Γ_{el}^{*} from motor side observer are shown in subplot (e). As can be seen the electrical torque, Γ_{el} varies to counteracts the torque applied to the shaft of the motor, Γ_L. In the steady state, the electrical torque is transmitted via the torsion spring to counteract the external load torque, Γ_{Le} applied to the load. It should be noted that the inner FDC speed control loop counteracts the real torque applied to the rotor, Γ_L but the external load torque, Γ_{Le}, still acts on the load mass. Proper operation of the load torque observer

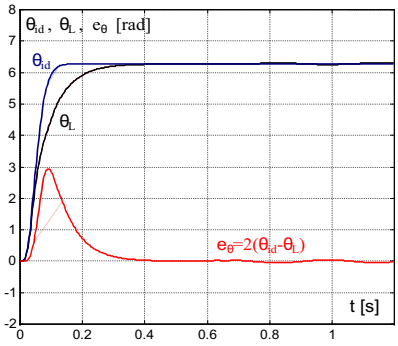

a) ideal and load position incl. error between them magnified 2x

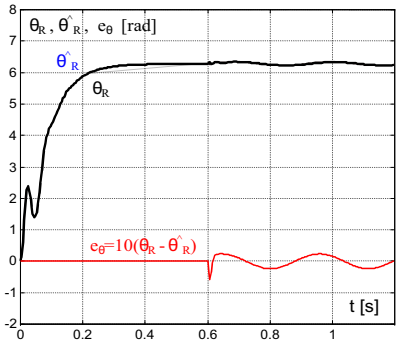

b) real and estimated rotor position incl. error between them magnified 10x

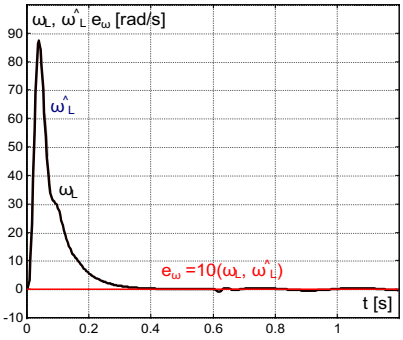

c) real and estimated load speed incl. error between them magnified 10x

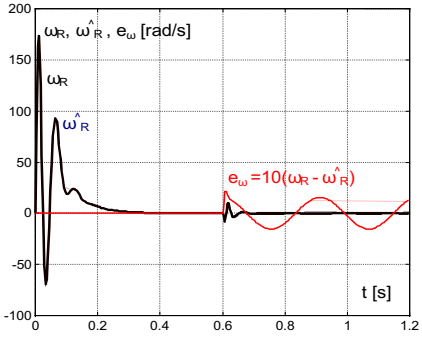

d) real and estimated rotor speed incl. error between them magnified 10x

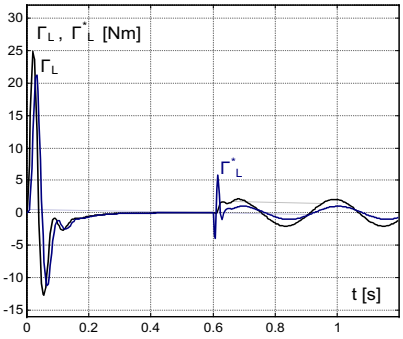

e) real and estimated load torque from motor side observer

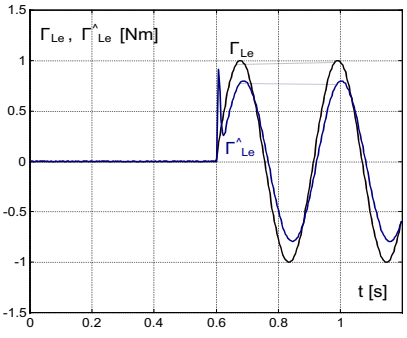

f) real and estimated external load torque from load side observer

Fig. 7. Simulation results for position control of the drive with PMSM and flexible coupling

is evident in subplot (f) where functions of applied load torque, Γ_{Le} together with ist estimate, $\Gamma^{\wedge}_{Le}$, follow each other. In spite of some departure from the ideal performance, the error between applied and estimated torque is mainly due to non-zero iteration interval and can be reduced if observer settling time, T_{so} is reduced.

5. Conclusion

A position control system based on principles of state-space control and forced dynamics control for electric drives with PMSM and flexible couplings between motor and load has been presented and verified by simulations. Implementation of two observers enables to eliminate position sensor on motor side. Presented simulations confirm that the derived position control algorithm is capable follow prescribed ideal position response with relatively small delay.

The designed observers on motor side and load side have non-oscillatory character and provide estimates of all state variables for control algorithm including external load force acting on the shaft of PMSM and load torque on the load side.

Developed control system is model based therefore further investigations should be carried out with regard to the parameters of motor and load mismatches. Due to prescribed speed dynamics the robustness of the FDC speed control system could be improved by adding an outer model reference adaptive control loop. The experimental implementation of the proposed load position control algorithm will follow as soon as possible.

References

1. Isidori A.: Nonlinear Control Systems, London, Springer-Verlag, UK, 1995.
2. Boldea I. and Nasar S.A.: Vector Control of AC Drives. 2nd edition, Boca Raton, FL., CRC Press, 1992.
3. Bose B. K.: Power Electronics and Variable Frequency Drives – Technology and applications, Institute of Electrical and Electronics Engineers, New York 1997.
4. Vittek J. and Dodds S. J.: Forced Dynamics Control of Electric Drives, Zilina, SK, EDIS, http://www.kves.uniza.sk, (E-learning), 2003, 20.10.2010r.
5. Vittek J., Bris P., Makys P. and Stulrajter M.: Forced dynamics control of PMSM drives with torsion oscillations. COMPEL, Vol. 29, No. 1, pp.188-205, 2010.
6. Zhang G. and Furusho J.: Speed control of two-inertia system by PI/PID control, IEEE Trans. on Industrial Electronics, vol. 47, No. 3, 2000, pp. 603-609.
7. Dodds S. J.: Settling Time Formulae for the Design of Control Systems with Linear Closed Loop Dynamics, in Proc. of the International Conf. AC&T‘07 – Advances in Computing and Technology, University of East London, UK, 2007.
8. Ohnishi K. and Morisawa M.: Motion control taking environmental information into account, in Proceedings of the EPE PEMC’02 International Conf., Cavtat, Croatia, 2002.
9. Dodds S. J. and Szabat K.: Forced Dynamic Control of Electric Drives with Vibration Modes in the Mechanical Load, in Proceedings of the International Conf. EPE-PEMC‘06, Portorož, Slovenia, 2006.

10. Brock S., Deskur J. and Zawirski K.: Robust Speed and Position Control of PMSM using Modified Sliding Mode Method, in Proceedings of the International Conf. EPE-PEMC'00, Kosice, Slovakia, vol. 6, pp. 6-29–6-34, 2000.
11. Comnat V., Cernat M., Moldoveanu F. and Ungar R.: Variable Structure Control of Surface Permanent Magnet Synchronous Machine, in Proceedings of the International Conf. PCIM'99 Nurnberg, Germany, pp. 351-356, 1999.
12. Perdukova D., Fedor P. and Timko J.: Modern Methods of Complex Drives Control, Acta Technica ČSAV, vol. 49, Prague, Czech Republic, pp. 31-45, 2004.
13. Brandstetter P.: AC Controlled Drives, Ostrava, Publishing Centre of VŠB TU, CZ (in Czech), 1999.
14. Aguilar O., Loukianov A. G. and Canedo J. M.: Observer-based Sliding Mode Control of Synchronous Motor, in Proceedings of the Intern. IFAC'02 Congress on Automatic Control, Guadalajara, Mexico, CD-Rom, 2002.
15. Szychta E., Szychta L., Kwiecień R., Figura R.: „Laboratorium z maszyn elektrycznych" podręcznik akademicki pod redakcją Leszka Szychta, Wydawnictwa Politechniki Radomskiej, Radom 2010, ISBN 978-83-7351-378-5.

The authors wish to thank for support to Slovak Grant Agency VEGA for funding this project.